



## Genome-wide association and HLA fine-mapping studies identify risk loci and genetic pathways underlying allergic rhinitis

**Waage, Johannes; Standl, Marie; Curtin, John A.; Jessen, Leon E.; Thorsen, Jonathan; Tian, Chao; Schoettler, Nathan; Flores, Carlos; Abdellaoui, Abdel; Ahluwalia, Tarunveer S.**

*Total number of authors:*  
52

*Published in:*  
Nature Genetics

*Link to article, DOI:*  
[10.1038/s41588-018-0157-1](https://doi.org/10.1038/s41588-018-0157-1)

*Publication date:*  
2018

*Document Version*  
Peer reviewed version

[Link back to DTU Orbit](#)

### *Citation (APA):*

Waage, J., Standl, M., Curtin, J. A., Jessen, L. E., Thorsen, J., Tian, C., Schoettler, N., Flores, C., Abdellaoui, A., Ahluwalia, T. S., Alves, A. C., Amaral, A. F. S., Antó, J. M., Arnold, A., Barreto-Luis, A., Baurecht, H., van Beijsterveldt, C. E. M., Bleecker, E. R., Bonàs-Guarch, S., ... AAGC collaborators (2018). Genome-wide association and HLA fine-mapping studies identify risk loci and genetic pathways underlying allergic rhinitis. *Nature Genetics*, 50(8), 1072-1080. <https://doi.org/10.1038/s41588-018-0157-1>

---

### General rights

Copyright and moral rights for the publications made accessible in the public portal are retained by the authors and/or other copyright owners and it is a condition of accessing publications that users recognise and abide by the legal requirements associated with these rights.

- Users may download and print one copy of any publication from the public portal for the purpose of private study or research.
- You may not further distribute the material or use it for any profit-making activity or commercial gain
- You may freely distribute the URL identifying the publication in the public portal

If you believe that this document breaches copyright please contact us providing details, and we will remove access to the work immediately and investigate your claim.

# Genome-wide association and HLA fine mapping studies identify risk loci and genetic pathways of allergic rhinitis

Johannes Waage<sup>1†</sup>, Marie Standl<sup>2†</sup>, John A Curtin<sup>3</sup>, Leon Jessen<sup>1</sup>, Jonathan Thorsen<sup>1</sup>, The 23andMe Research Team<sup>4</sup>, AAGC collaborators<sup>4</sup>, Abdel Abdellaoui<sup>5</sup>, Tarunveer S Ahluwalia<sup>1</sup>, Alexander Alves<sup>6</sup>, Andre F S Amaral<sup>7</sup>, Josep Maria Antó<sup>8</sup>, Andreas Arnold<sup>9</sup>, Carlos Flores<sup>10,30</sup>, Hansjörg Baurecht<sup>11</sup>, Toos CEM Beijsterveldt<sup>5</sup>, Eugene R. Bleeker<sup>12</sup>, Silvia Bonàs-Guarch<sup>13</sup>, Dorret Boomsma<sup>5,14</sup>, Susanne Brix<sup>15</sup>, Supinda Bunyavanich<sup>16</sup>, Esteban Burchard<sup>17,18</sup>, Zhanghua Chen<sup>19</sup>, Ivan Curjuric<sup>20,21</sup>, Adnan Custovic<sup>22</sup>, Martijn den Dekker<sup>23,24,25</sup>, Shyamali C. Dharmage<sup>26</sup>, Julia Dmitrieva<sup>27</sup>, Liesbeth Duijts<sup>23,24,25,28</sup>, Markus Ege<sup>29</sup>, Amalia Barreto-Luis<sup>10</sup>, W. James Gauderman<sup>19</sup>, Michel Georges<sup>27</sup>, Christian Gieger<sup>31,32</sup>, Frank Gilliland<sup>19</sup>, Raquel Granell<sup>33</sup>, Hongsheng Gui<sup>34</sup>, Torben Hansen<sup>35</sup>, Joachim Heinrich<sup>2,36</sup>, John Henderson<sup>33</sup>, Natalia Hernandez-Pacheco<sup>10,37</sup>, David A. Hinds<sup>38</sup>, David Hinds<sup>38</sup>, Patrick Holt<sup>39</sup>, Medea Imboden<sup>20,21</sup>, Vincent Jaddoe<sup>23,24,25</sup>, Marjo-Riita Jarvelin<sup>6</sup>, Deborah L Jarvis<sup>7</sup>, Kamilla K Jensen<sup>40</sup>, Ingileif Jónsdóttir<sup>41,42</sup>, Michael Kabesch<sup>43</sup>, Jaakko Kaprio<sup>44,45,46</sup>, Ashish Kumar<sup>47,48,49</sup>, Young-Ae Lee<sup>50,51</sup>, Albert M Levin<sup>52</sup>, Xingnan Li<sup>53</sup>, Fabian Lorenzo-Diaz<sup>37</sup>, Erik Melén<sup>47,54</sup>, Josep Maria Mercader<sup>13,55,56</sup>, Deborah A. Meyers<sup>12</sup>, Rachel Myers<sup>57</sup>, Dan L. Nicolae<sup>57</sup>, Ellen Nohr<sup>58</sup>, Teemu Palviainen<sup>45</sup>, Lavinia Paternoster<sup>59</sup>, Lavinia Paternoster<sup>59</sup>, Craig Pennell<sup>60</sup>, Göran Pershagen<sup>47,61</sup>, Maria Pino-Yanes<sup>10,30,37</sup>, Nicole M Probst-Hensch<sup>20,21</sup>, Franz Rüschenhoff<sup>60</sup>, Nathan Schoettler<sup>57</sup>, Angela Simpson<sup>3</sup>, Kari Stefansson<sup>41,42</sup>, Jordi Sunyer<sup>8</sup>, Gardar Sveinbjörnsson<sup>41</sup>, Elisabeth Thiering<sup>2,62</sup>, Philip J. Thompson<sup>63</sup>, Chao Tian<sup>38</sup>, Chao Tian<sup>38</sup>, Maties Torrent<sup>64</sup>, David Torrents<sup>13,65</sup>, Joyce Y. Tung<sup>38</sup>, Carol Wang<sup>60</sup>, Stephan Weidinger<sup>11</sup>, Scott Weiss<sup>66</sup>, Gonneke Willemsen<sup>5</sup>, L Keoki Williams<sup>34,67</sup>, Carole Ober<sup>57</sup>, Manuel A. Ferreira<sup>68</sup>, Hans Bisgaard<sup>1</sup>, David Strachan<sup>69</sup>, Klaus Bønnelykke<sup>1</sup>

Corresponding author: Hans Bisgaard<sup>1</sup>

<sup>1</sup>COPSAC, Copenhagen Prospective Studies on Asthma in Childhood, Herlev and Gentofte Hospital, University of Copenhagen, Copenhagen, Denmark. <sup>2</sup>Institute of Epidemiology I, Helmholtz Zentrum München - German Research Center for Environmental Health, Neuherberg, Germany. <sup>3</sup>Centre for Respiratory Medicine and Allergy, Institute of Inflammation and Repair, University of Manchester and University Hospital of South Manchester, Manchester Academic Health Sciences Centre, Manchester, UK. <sup>4</sup>To be listed in Supplementary Information. <sup>5</sup>Dept Biological Psychology, Netherlands Twin Register, VU University, Amsterdam. <sup>6</sup>Department of Epidemiology and Biostatistics, School of Public Health, Imperial College, London, UK. <sup>7</sup>Population Health and Occupational Disease, National Heart and Lung Institute, Imperial College London, London, UK. <sup>8</sup>ISGlobal-Center for Research in Environmental Epidemiology (CREAL), Universitat Pompeu Fabra (UPF), CIBER Epidemiología y Salud Pública (CIBERESP), Barcelona, Spain. <sup>9</sup>Clinic and Polyclinic of Dermatology, University Medicine Greifswald, Greifswald, Germany. <sup>10</sup>Research Unit, Hospital Universitario N.S. de Candelaria, Universidad de La Laguna, Tenerife, Spain. <sup>11</sup>Department of Dermatology, Venereology and Allergology, University-Hospital Schleswig-Holstein, Campus Kiel, Kiel, Germany. <sup>12</sup>Divisions of Pharmacogenomics and Genetics, Genomics and Precision Medicine, Department of Medicine, University of Arizona College of Medicine, Tucson, AZ, USA. <sup>13</sup>Barcelona Supercomputing Center (BSC). Joint BSC-CRG-IRB Research Program in Computational Biology, Barcelona, Spain. <sup>14</sup>EMGO Institute for Health and Care Research. <sup>15</sup>Department of Biotechnology and Biomedicine, Technical University of Denmark, Kgs. Lyngby, Denmark. <sup>16</sup>Department of Genetics and Genomic Sciences, Icahn School of Medicine at Mount Sinai, New York, NY, USA. <sup>17</sup>Department of Medicine, University of California San Francisco, San Francisco, California, USA. <sup>18</sup>Department of Bioengineering & Therapeutic Sciences, University of California San Francisco, San Francisco, California, USA. <sup>19</sup>Dept of Preventive Medicine, University of Southern California, Keck School of Medicine. <sup>20</sup>University of Basel, Switzerland. <sup>21</sup>Swiss Tropical and Public Health Institute, Basel, Switzerland. <sup>22</sup>Department of Paediatrics, Imperial College London, UK. <sup>23</sup>The Generation R Study Group. <sup>24</sup>Department of Pediatrics, division of Respiratory Medicine. <sup>25</sup>Department of Epidemiology, Erasmus Medical Center, Rotterdam, the Netherlands. <sup>26</sup>Melbourne School of Population and Global Health, University of Melbourne, Melbourne, Australia. <sup>27</sup>Laboratory of Animal Genomics, Unit of Medical Genomics, GIGA Institute, University of Liège, Belgium. <sup>28</sup>Department of Pediatrics, division of Neonatology. <sup>29</sup>LMU Munich, Dr von Hauner Children's Hospital, Munich and German Center for Lung Research (DZL), Munich, Germany. <sup>30</sup>CIBER de Enfermedades Respiratorias (CIBERES), Instituto de Salud Carlos III, Madrid, Spain. <sup>31</sup>Research Unit of Molecular Epidemiology, Helmholtz Zentrum München-German Research Center for Environmental Health, Neuherberg, Germany. <sup>32</sup>Institute of Epidemiology II, Helmholtz Zentrum München-German Research Center for Environmental Health, Neuherberg, Germany. <sup>33</sup>School of Social and

Community Medicine, University of Bristol, UK. <sup>34</sup>Center for Health Policy and Health Services Research, Henry Ford Health System, Detroit, MI, USA. <sup>35</sup>Novo Nordisk Foundation Center for Basic Metabolic Research, Section of Metabolic Genetics, Department of Health and Medical Sciences, University of Copenhagen, Copenhagen, Denmark. <sup>36</sup>Institute and Outpatient Clinic for Occupational, Social and Environmental Medicine, University of Munich Medical Center, Ludwig-Maximilians-Universität München, Munich, Germany. <sup>37</sup>Genomics and Health Group, Department of Biochemistry, Microbiology, Cell Biology and Genetics, Universidad de La Laguna, La Laguna, Tenerife, Spain. <sup>38</sup>23andMe, Inc., Mountain View, California, USA. <sup>39</sup>Telethon Kids Institute (TKI), Perth Australia. <sup>40</sup>Department of Bioinformatics, Technical University of Denmark, Kgs. Lyngby, Denmark. <sup>41</sup>deCODE genetics / Amgen Inc, Reykjavik, Iceland. <sup>42</sup>Faculty of Medicine, University of Iceland, Reykjavik, Iceland. <sup>43</sup>Department of Pediatric Pneumology and Allergy, University Children's Hospital Regensburg (KUNO), Regensburg, Germany. <sup>44</sup>Department of Public Health, University of Helsinki, Helsinki, Finland. <sup>45</sup>Institute for Molecular Medicine Finland FIMM, University of Helsinki, Helsinki, Finland. <sup>46</sup>National Institute for Health and Welfare, Helsinki, Finland. <sup>47</sup>Institute of Environmental Medicine, Karolinska Institutet, Stockholm, Sweden. <sup>48</sup>Department of Public Health Epidemiology, Unit of Chronic Disease Epidemiology, Swiss Tropical and Public Health Institute, Basel, Switzerland. <sup>49</sup>University of Basel, Basel, Switzerland. <sup>50</sup>Max-Delbrück-Center (MDC) for Molecular Medicine, Berlin, Germany. <sup>51</sup>Clinic for Pediatric Allergy, Experimental and Clinical Research Center, Charité Universitätsmedizin Berlin, Germany. <sup>52</sup>Department of Public Health Sciences, Henry Ford Health System, Detroit, MI, USA. <sup>53</sup>Divisions of Genetics, Genomics and Precision Medicine, Department of Medicine, University of Arizona College of Medicine, Tucson, AZ, USA. <sup>54</sup>Sachs' Children's Hospital, Stockholm, Sweden. <sup>55</sup>Programs in Metabolism and Medical & Population Genetics, Broad Institute of Harvard and MIT, Cambridge, Massachusetts, USA. <sup>56</sup>Diabetes Unit and Center for Genomic Medicine, Massachusetts General Hospital, Boston, Massachusetts, USA. <sup>57</sup>Department of Human Genetics, University of Chicago, Chicago IL, USA. <sup>58</sup>Institute of Clinical Research, University of Southern Denmark, Department of Obstetrics & Gynecology, Odense University Hospital, Odense, Denmark. <sup>59</sup>MRC Integrative Epidemiology Unit at the University of Bristol, School of Social and Community Medicine, University of Bristol, UK. <sup>60</sup>Division of Obstetrics and Gynaecology, The University of Western Australia (UWA), Perth, Australia. <sup>61</sup>Centre for Occupational and Environmental Medicine, Stockholm County Council, Stockholm. <sup>62</sup>Ludwig-Maximilians-University of Munich, Dr. von Hauner Children's Hospital, Division of Metabolic Diseases and Nutritional Medicine, Munich, Germany. <sup>63</sup>Institute for Respiratory Health, Harry Perkins Institute of Medical Research, University of Western Australia, Nedlands, Australia. <sup>64</sup>ib-salut, Area de Salut de Menorca, Menorca, Spain. <sup>65</sup>Institució Catalana de Recerca i Estudis Avançats (ICREA), Barcelona, Spain. <sup>66</sup>Channing Division of Network Medicine, Brigham & Women's Hospital and Harvard Medical School, Boston, MA, USA. <sup>67</sup>Department of Internal Medicine, Henry Ford Health System, Detroit, MI, USA. <sup>68</sup>QIMR Berghofer Medical Research Institute, Brisbane, Queensland, Australia. <sup>69</sup>Population Health Research Institute, St George's, University of London, London, UK.

†These authors contributed equally to this work

## Introduction

Allergic rhinitis is the most common clinical presentation of allergy, affecting 400 million people worldwide, and with increasing incidence in westernized countries.<sup>1,2</sup> To elucidate the genetic architecture and understand disease mechanisms of allergic rhinitis, we carried out a meta-analysis of allergic rhinitis in 59,762 cases and 152,358 controls of European ancestry and identified a total of 41 risk loci for allergic rhinitis, including 20 loci not previously associated with allergic rhinitis, which were confirmed in a replication phase of 60,720 cases and 618,527 controls. Functional annotation implied genes involved in various immune pathways, and fine mapping of the HLA region suggested amino acid variants of importance for antigen binding. We further performed GWASs of allergic sensitization against inhalant allergens and non-allergic rhinitis suggesting shared genetic mechanisms across rhinitis-related traits. Future studies of the identified loci and genes might identify novel targets for treatment and prevention of allergic rhinitis.

## Main text

Allergic rhinitis (AR) is an inflammatory disorder of the nasal mucosa mediated by allergic hypersensitivity responses to environmental allergens<sup>1</sup> with large adverse effects on quality of life and health care expenditures. The underlying causes for AR are still not understood and prevention of the disease is not possible. The heritability of AR is estimated to be more than 65%<sup>3,4</sup>. Seven loci have been associated and with allergic rhinitis in genome-wide association studies (GWAS) of AR per se, while other have been suggested from GWAS studies on related traits, such as self-reported allergy, asthma plus hay fever, or allergic sensitization<sup>5-9</sup>, but only few of these have been replicated. We carried out a large-scale meta-GWAS of AR including a discovery meta-analysis of 16,531,985 genetic markers from 18 studies comprising 59,762 cases and 152,358 controls of primarily European ancestry (**Supplementary Table 1**, cohort recruitment details in **Supplementary Note**). We report the genetic heritability on the liability scale of AR as at least 7.8% (assuming 10% disease prevalence), with a genomic inflation of 1.048 (**Supplementary Figure 1**). We identified 42 genetic loci, with index markers below genomewide significance ( $p < 5e-8$ ), of which 21 have previously been reported in relation to AR or other inhalant allergy<sup>6-9</sup> (**Fig. 1, Table 1, Supplementary Fig. 2, Supplementary Fig. 3**). One study (23andMe) had a proportionally large weight (~80%) in the discovery phase. Overall there was good agreement between 23andMe and the other studies with respect to effect size and direction, and regional association patterns (**Supplementary Table 2 and Supplementary Fig. 4+5**), and the genetic correlation was 0.80 ( $p < 2e-17$ ). Heterogeneity between 23andMe and the remaining studies was statistically significant ( $p < 0.05$ ) for 7 of 42 loci, in most cases due to a smaller effect size in 23andMe. This was likely due to many non-23andMe studies using a more robust phenotype definition of doctor diagnosed AR (**Supplementary Table 3**), which tended to result in larger effect sizes (**Supplementary Table 4**).

The index markers from a total of 25 loci that had not previously been associated with AR or other inhalant allergy were carried forward to the replication phase. These included 16 loci that showed genome-wide significant association in the discovery phase and evidence of association ( $p < 0.05$ ) in both 23andMe and non-23andMe studies (**Supplementary Table 2**), and an additional 9 loci that were selected from the p-value stratum between  $5 \times 10^{-8}$  and  $1 \times 10^{-6}$  based on enrichment of gene sets involved in immune-signalling (**Supplementary Table 5**). Replication was sought in another 10 studies with 60,720 cases and 618,527 controls. Of the 25 loci, 20 loci reached a Bonferroni-corrected significance threshold of 0.05 ( $p < 0.0019$ ) in a meta-analysis of replication studies (**Fig. 1 (blue), Table 1**), and all of these reached genome-wide significance in the combined fixed-effect meta-analysis of discovery and replication studies (**Table 1**). Evidence of heterogeneity was seen for one of these loci (rs1504215), which did not reach statistical significance in the random effects model (0.95 [0.92; 0.97],  $p = 2.83 \times 10^{-7}$ , **Supplementary Fig. 3**).

A conditional analysis of top loci identified 13 additional independent variants at  $p < 1 \times 10^{-5}$ , with 4 of these being genome-wide significant (near *WDR36*, *HLA-DQB1*, *IL1RL1* and *LPP*) (**Supplementary Table 6** and **Supplementary Fig. 5**, bottom panel).

To gain insight into functional consequences of known and novel loci, we utilised a number of data sources, including 1) 11 eQTL sets and 1 meQTL set from blood and blood subsets; 2) 2 eQTL sets and 1 meQTL set from lung tissue; and 3) data on enhancer-promoter interactions in 15 different blood subsets. Support of regulatory effects on coding genes was found for 33 out of the 41 loci. Many loci showed evidence of regulatory effects across a wide range of immune cell types (including B- and T-cells), while other seemed cell type-specific, like e.g. innate lymphoid cells (**Table 2** and **Supplementary Table 7**). Calculation of the “credible set” of markers for each locus using a Bayesian approach that selects markers likely to contain the causal disease-associated markers (**Supplementary Table 8**) and looking up these in the Variant Effect Predictor database generated a list of 17 markers producing amino acid changes, including deleterious changes in NUSAP1, SULT1A1 and PLCL, as predicted by SIFT (**Supplementary Table 9**).

The major histocompatibility complex on chr6p harbored some of the strongest association signals in the GWAS with 2 independent signals located around *HLA-DQB* and *HLA-B*, respectively. The top variant at *HLA-DQB* was an eQTL for several HLA-genes, including *HLA-DQB1*, *HLA-DQA1*, *HLA-DQA2*, and *HLA-DRB1* in immune and/or lung tissue, and the top variant at *HLA-B* was an eQTL for *MICA* (**Supplementary Table 7**). In addition we found highly significant associations with several well imputed amino acid variants (**Supplementary Tables 10 and 11**). Importantly, the strongest associated amino acid variants in *HLA-DQB1* and *HLA-B*, respectively (**Supplementary Table 10**) were both located in the peptide binding pockets with a high likelihood of affecting MHC-peptide interaction (**Figure 2**). MHC class II molecules, including *HLA-DQ*, are known for their role in allergen-binding and Th2 driven immune responses.<sup>10</sup> The strong association with *HLA-DQB1 His30* ( $p = 2.06 \times 10^{-28}$ , OR=0.91) in the peptide binding pocket, and the moderate LD ( $r^2 = 0.71$ ) with the GWAS top SNP rs3400401, therefore suggest that the association signal at this locus involves changes in allergen binding properties by *HLA-DQ* and thereby altered risk of allergen-specific immunity. We also found association with several classical HLA alleles, including *HLA-DQB1\*02:02*, *HLA-DQB1\*03:01*,

HLA-DRB1\*04:01, and HLA-C\*04:01, which were in weak LD ( $r^2 < 0.1$ ) with the GWAS top SNPs (**Supplementary Tables 12 and 13**). These findings suggest that genetic associations in HLA-MHC region both involve variants affecting gene regulation and structure, similar to what has been found for autoimmune disease.<sup>11,12</sup>

The majority of the 20 loci not previously associated with AR per se imply genes with a known role in the immune system, including IL7R<sup>13, 14</sup>, SH2B3<sup>15</sup>, CEBPA/CEBPG<sup>16, 17</sup>, CXCR5<sup>18</sup>, FCER1G, NFKB1<sup>19</sup>, BACH2<sup>20, 21</sup>, TYRO3<sup>22</sup>, LTK<sup>23</sup>, VPRBP<sup>24</sup>, SPPL3<sup>25</sup>, OASL<sup>26</sup>, RORA<sup>27</sup>, and TNFSF11<sup>28</sup>. Other loci imply genes with no clear function in AR pathogenesis. These include one of the strongest associated loci in this meta-analysis at 12q24.31 with the top-signal located between CDK2AP1 and C12orf65, harboring cis-eQTLs in blood and lung tissue for several genes and evidence for enhancer-promoter interaction with DDX55 in various immune cells. (Table 2 and further locus description in the Supplementary Note). Concomitantly with the current study, a GWAS combining asthma, eczema and AR was conducted.<sup>29</sup> The majority (15/20) of identified AR loci in our study were also suggested in the previous, more unspecific, GWAS<sup>29</sup> (as indicated in Tables 1 and 2), while many suggested loci from the previous GWAS were not identified in our study. Asthma, eczema and allergic rhinitis are related but distinct disease entities, often with separate disease mechanisms, e.g. allergic sensitization is present in only 50% of children with asthma<sup>30</sup> and 35% of children with eczema.<sup>31</sup> Our results therefore complement those from the less specific “atopic phenotype” GWAS<sup>29</sup> by pinpointing loci specifically associated, and replicated, in relation to allergic rhinitis.

AR loci were significantly enriched ( $p < 1e-5$ ) for variants reported to be associated with autoimmune disorders. Reported autoimmune variants were located within a 1mb distance of 31 (76%) of the 41 AR loci. For 24 of these, an autoimmune top SNP was also associated with AR, and for 12 of these the autoimmune top SNP was in LD ( $r^2 > 0.5$ ) with the AR top SNP (**Supplementary Table 14**). For approximately half of these, the direction of effect was the same for the autoimmune and AR top SNP in line with a previous study,<sup>32</sup> underlining the complex genetic relationship between AR and autoimmunity, which might involve shared as well as diverging molecular mechanisms.

Assessment of enrichment of AR-associated variant burden in open chromatin as defined by DNase hypersensitive sites showed a clear enrichment in several blood and immune cell subsets, with the largest enrichment in T-cells (CD3 expressing), B-cells (CD19 expressing), and T and NK-cells (CD56-expressing) (**Fig. 3, Supplementary Table 15, Supplementary Fig. 6**). We also probed tissue enrichment by means of gene expression data from a wide number of sources, showing enrichment of AR genes in blood and immune cell subsets, as well as in tissues of the respiratory system, including oropharynx, respiratory and nasal mucosa (**Supplementary Table 16**).

To explore biological connections and identify new pathways associated with AR, we combined all genes suggested from eQTL/meQTL analyses, enhancer-promoter interactions and localization within the top loci. The resultant prioritized gene set consisted of 255 genes, of which 89 (~36%) were present in more than one set (**Supplementary Fig. 7**). Overall, the full set was enriched for pathways involved in Th1 and Th2 Activation (**Fig. 4**), antigen presentation, cytokine signaling, and inflammatory responses (**Supplementary Table 17**).



Using the 255 prioritized genes in combination with STRING to identify proteins that interact with the proteins encoded by the high priority genes, we demonstrated a high degree of interaction at the protein level, and several of these proteins are target of approved drugs or drugs in development, including TNFSF11, NDUFAF1, PD-L1, IL-5, and IL-13 (**Fig. 4**). AR is strongly correlated to allergic sensitization (presence of allergen-specific IgE), but sensitization is often present without AR suggesting specific mechanisms determining progression from sensitization to disease. We therefore conducted a GWAS on sensitization to inhalant allergens (AS) comprising 8,040 cases and 16,441 controls from 13 studies (**Supplementary Table 1**), making it the largest GWAS on allergic sensitization to date<sup>7</sup>. A total of 10 loci reached genome-wide significance, including one novel hit near the *FASLG* gene (**Supplementary Table 18**). The genetic heritability on the liability scale was 17.75% (10% prevalence), considerably higher than the heritability of AR in consistency with a more homogeneous phenotype. Look-up of AR top-loci in the AS GWAS demonstrated large agreement with 39 of the 41 AR markers showing same direction of effect and 28 also showing nominal significance for AS (**Supplementary Table 19**). This suggests that AR and AS share biological mechanisms and that AS loci generally affect systemic allergic sensitization. We compared genetic pathways of AR and AS using the DEPICT tool showing overlap in enriched pathways but also differences among the top gene sets, with AR gene sets characterized by B-cell, Th2, and parasite responses and AS gene sets characterized by a broader activation of cells (**Supplementary Fig 8 and Supplementary Tables 20 and 21**).

Non-allergic rhinitis, defined as rhinitis symptoms without evidence of allergic sensitization, is a common but poorly understood disease entity.<sup>33</sup> We performed the first GWAS on this phenotype hypothesizing that this might reveal specific rhinitis mechanisms. The analysis included 2,028 cases and 9,606 controls from 9 studies but did not identify any risk loci at the genome-wide significance level. Comparison with AR results suggested some overlap in susceptibility loci (**Supplementary Note and Supplementary Table 22**).

We estimated the proportion of AR in the general population that can be attributed to the 41 identified AR loci and obtained a conservative population-attributable risk fraction estimate of 39% (95% CI 26%-50%), considering the 10% of the population with the lowest genetic risk scores to represent an 'unexposed' group. Allergic rhinitis prevalence plotted by genetic risk score (**Supplementary Fig. 9**) showed approximately 2 times higher prevalence in the 7% of the population with the highest risk score compared to the 7% with the lowest risk score. Finally, we investigated the genetic correlation of AR with AS, asthma<sup>34</sup>, and eczema<sup>35</sup> by LD score regression. There was a strong correlation between AR and AS ( $r^2=0.73$ ,  $p<2e-34$ ), moderate with asthma ( $r^2=0.60$ ,  $p<3e-14$ ) and weaker with eczema ( $r^2=0.40$ ,  $p<2e-07$ ).

In conclusion, we expanded the number of established susceptibility loci for AR and highlighted involvement of AR susceptibility loci in diverse immune cell types and both innate and adaptive IgE-related mechanisms. Future studies of novel AR loci might identify targets for treatment and prevention of disease.

## Methods:

### Phenotype definition

#### Allergic rhinitis (AR)

Cases were defined as individuals ever having a diagnosis or symptoms of AR dependant on available phenotype definitions in the included studies (**Supplementary Table 3** and cohort recruitment details in **Supplementary Note**). To maximize numbers and optimize statistical power, we did not require doctor-diagnosed AR or verification by allergic sensitization. This approach was confirmed by a sensitivity analysis in 23andMe based on association with known risk loci for allergic rhinitis (data not shown). Controls were defined as individuals who never had a diagnosis or symptoms of AR.

#### Allergic sensitization (AS)

We considered specific IgE production against inhalant allergens without restriction by assessment method or type of inhalant allergen. Cases were defined as individuals with objectively measured sensitization against at least one of the inhalant allergens tested for in the respective studies, and controls were defined as individuals who were not sensitized against any of the allergens tested for. We included sensitization assessed by skin reaction after puncture of the skin with a droplet of allergen extract (SPT) and/or by detection of the levels of circulating allergen-specific IgE in the blood. The SPT wheal diameter cutoffs were 3 mm larger than the negative control for cases and smaller than 1 mm for controls. To optimize case specificity and the correlation between methods, we chose a high cutoff of specific IgE levels for cases (0.7 IU/ml) and a low cutoff for controls (0.35 IU/ml).

#### Non-allergic rhinitis (NAR)

Cases were defined as individuals with current allergic rhinitis symptoms (within the last 12 months) and no allergic sensitization (negative specific IgE ( $< 0.35$  IU/mL) and/or negative skin prick test ( $< 1$  mm) for all allergens and time points tested)

Controls were defined as individuals never having symptoms of allergic rhinitis and no allergic sensitization (negative specific IgE ( $< 0.35$  IU/mL) and/or negative skin prick test ( $< 1$  mm) for all allergens and time points tested)

For all 3 phenotypes, we combined data from children and adults but chose a lower age limit of 6 years, as allergic rhinitis and sensitization status at younger ages show poorer correlation with status later in life, both owing to transient symptoms/sensitization status and frequent development of symptoms/sensitization during late childhood.

### GWAS QC and cohort summary data harmonization

For AR, AS, and NAR, each cohort imputed their data separately using the 1000 Genomes Project (1KGP) phase 1, version 3 release, and conducted the genome-wide association analysis adjusted for sex and if necessary for age and principal components (Supplementary



Table COHORTS). All studies included individuals of European descent, except Generation R and RAINE, comprising a mixed, multi-ethnic population. We utilized EasyQC v. 9.2<sup>36</sup> for quality control and marker harmonization for cohort-level meta-GWAS summary files. Cohort data was harmonized to genome build GRCh37 and checked against 1KGP phase 3 reference allele frequencies for processing problems. GWAS summary “karyograms” were visually inspected to catch cohorts with incomplete data. Distributions of estimate coefficients and errors, as well as “Standard error vs. sample size”- and “p value vs. z-score” plots were inspected for each cohort for systematic errors in statistical models. Ambiguous markers that were non-unique in terms of both genomic position and allele coding were removed. A minimum imputation score of 0.3 ( $R^2$ ) or 0.4 (proper\_info) was required for markers. A minimum minor allele count of 7 was required for each marker in each cohort, as suggested by the GIANT consortium and EasyQC.

## Meta-Analysis

For AR, AS, and NAR, meta-analysis for the discovery phase was conducted using GWAMA<sup>37</sup> with an inverse variance weighted fixed-effect model with genomic control correction of the individual studies. Each locus is represented by the variant showing the strongest evidence within a 1Mb buffer. Loci were inspected visually by plotting genomic neighbourhood and coloring for 1KGP  $r^2$  values. From the pool of genomewide significant markers in the discovery, one locus with index marker rs193243426 without a credible LD structure was removed from further analysis (**Supplementary Fig. 10**). Heterogeneity was assessed with Cochran’s Q test. Meta-analysis of replication candidates from the AR discovery phase was carried out using R version 3.4.0, and the *meta* package version 4.8-2 with an inverse variance weighted fixed-effect model. For a subset of markers, cohorts reported suitable proxies ( $r^2 > 0.85$ ), where followed-up markers were not present or had insufficient imputation or genotyping quality (**Supplementary Table 23**).

## Gene set overrepresentation analysis, discovery phase

To facilitate selection of biologically relevant discovery candidates in the sub-genomewide significant stratum ( $5e-8 < p < 1e-6$ ), we employed a custom gene set overrepresentation analysis algorithm implemented in R, with a scoring and permutation regime modelled after MAGENTA.<sup>38</sup> Genes with lengths less than 200bp, with copies on multiple chromosomes, and with multiple copies on the same chromosome more than 1Mb apart were removed from analysis. Gene models (GENCODE v 19) were downloaded from the UCSC Table Browser,<sup>39</sup> and expanded 110 kb upstream, and 40 kb downstream, similar to MAGENTA. The HLA region was excluded from analysis (chromosome 6: 29,691,116-33,054,976). Similar to MAGENTA, gene scores were adjusted for number of markers per gene, gene width, recombination hotspots, genetic distance, and number of independent markers per gene, all with updated data from UCSC Table Browser. For the gene set overrepresentation permutation calculation, gene sets from the MSigDB collections c2, c3, c5, c7, and hallmark, were included.<sup>40</sup> A MAGENTA-style enrichment cutoff at 95% was used. Gene sets with  $FDR < 0.05$  were considered.

## Conditional analyses

To identify additional independent markers at each discovery genomic region, we used Genome-wide Complex Trait Analysis (GCTA) v. 1.26.0.<sup>41</sup> Within a window of +/- 1Mb of each discovery phase index marker, all markers were conditioned on the index using the --cojo-cond feature of GCTA with default parameters. Plink v. v1.90b3.42<sup>42</sup> was used to calculate  $r^2$  for GCTA with the UK10K full genotype panel<sup>43</sup> as reference. A total of 42 of 52 markers from the full discovery phase were present in UK10K. As a MAF-dependent inflation of conditional p-values was observed (data not shown), only conditional markers with MAF  $\geq$  10% were selected.

## Locus definition and credible sets for VEP annotation

Discovery loci were defined as index markers extended with markers in LD ( $r^2 \geq 0.5$ ), based on the 1KGP phase 3. Protein coding gene transcript models (GENCODE V24) were downloaded from the UCSC Table Browser, and nearest upstream, downstream, as well as all genes within the extended loci were annotated.

Credible sets for each locus were calculated using the method of Morris, A.P.<sup>44</sup>.

LD was calculated for each discovery index variant within +/- 500 kb, and markers with  $r^2 < 0.1$  were excluded. For the remaining markers, the Bayesian Factor (ABF) values and the posterior probabilities (PostProb) were calculated, and cumulative posterior probability values were generated based ranking markers on ABF. Finally, variants were included in the 99% credible set until the cumulative posterior probability was greater or equal than 0.99.

Credible sets for each loci was annotated with information on mutation impact in coding regions using the Variant effect Prediction (VeP) REST API<sup>45</sup>, exporting only the nonsynonymous substitutions.

## GWAS catalogue lookup

For annotation of markers with identification in previous GWA studies, the GWAS catalog was downloaded from NHGRI-EBI (v.1.0.1, 2016-11-28). For this analysis, AR loci were lifted from genomic build GRCh37 to GRCh38, and extended with +/- 1Mb in each direction before being overlapped with GWAS catalog annotations. Relevant GWAS catalog overlap traits were binned into trait groups "Allergic Rhinitis", "Asthma", "Autoimmune", "Eczema", "Infectious Diseases", "Lung-related Traits", and "Other allergy". A million random genomic intervals of the same length (2Mb) were obtained to generate a background overlap distribution, and p-values were calculated from this background.

## HLA classical allele analysis

Analyses of imputed classical HLA-alleles were performed in the 23andMe study (AR discovery population) comprising 49,180 individuals with allergic rhinitis and 124,102 controls.

HLA imputation was performed with HIBAG.<sup>46</sup> We imputed allelic dosage for HLA-A, B, C, DPB1, DQA1, QB1, and DRB1 loci at four-digit resolution using the default settings of HIBAG for a total of 292 classical HLA alleles.

Using an approach suggested by P. de Bakker,<sup>47</sup> we downloaded the files that map HLA alleles to amino acid sequences from <https://www.broadinstitute.org/mpg/snp2hla/> and mapped our imputed HLA alleles at four-digit resolution to the corresponding amino acid sequences; in this way we translated the imputed HLA allelic dosages directly to amino acid dosages. We encoded all amino acid variants in the 23andMe European samples as 2395 bi-allelic amino acid polymorphisms as previously described.<sup>48</sup>

Similar to the SNP imputation, we measured imputation quality using  $r^2$ , which is the ratio of the empirically observed variance of the allele dosage to the expected variance assuming Hardy-Weinberg equilibrium.

To test associations between imputed HLA alleles, amino acid variants, and phenotypes, we performed logistic regression using the same set of covariates used in the SNP-based GWAS. We applied a forward stepwise strategy, within each type of variant, to establish statistically independent signals in the HLA region. Within each variant type, we first identified the most strongly associated signals (lowest p-value) and performed forward iterative conditional regression to identify other independent signals. All analyses were controlled for sex and five principal components of genetic ancestry. The p-values were calculated using a likelihood ratio test.

## Structural visualization of amino acid variants

Structural visualization of amino acid variants was performed for the strongest associated variants in HLA-DQB1 (position 30) and HLA-B (position 116), respectively (**Supplementary Table 10**) and were made using X-ray structures from Protein Data Bank (PDB).<sup>49</sup> To find the best structure we used the specialized search function in the Immune Epitope Database,<sup>50</sup> selecting only X-ray crystalized structures for the specific MHC type HLA-DQB1 and HLA-B. Using this criterion, we found 17 crystallized structures for HLA-DQB1 and 164 structures for HLA-B. From these lists, we selected the structure with the lowest resolution and the amino acids encoded by the reported top SNPs. The PDB accession code for the selected structures was 4MAY<sup>51</sup> for HLA-DQB1 and 2A83<sup>52</sup> for HLA-B and both structures were visualized using PyMOL (<http://www.pymol.org>). Furthermore, we used PyMOL to measure intra-molecular distances from the side chain of the amino acids associated with allergic rhinitis to the C atoms in the peptide. This distance measure was chosen to accommodate the possibility for different amino acids in the peptide. In order for two amino acids to interact the distance should be approximately 4Å or less. We measured distances of 6Å (HLA-DQB1) and 7Å (HLA-B), however these distances do not include the peptide side chains which range from 1.5 Å – 8.8 Å. Therefore, we estimate that physical interaction between the amino acids encoded by the top SNPs and the peptide is likely.

## Genetic heritability and genetic correlation

For calculating genetic heritability and genetic correlation between AR and AS, as well as between clinical cohorts and 23andMe within AR, we utilized the LD score regression based method as implemented by LDSC v.1.0.<sup>45,53</sup> Population prevalence was set to 10% for AR and

AS. Genetic correlation analysis between AR, AS and published GWAS studies was carried out using the LDHUB platform v1.3.1<sup>54</sup> against all traits, but excluding Metabolites<sup>55</sup>.

## eQTL sources and analysis

From GTEx V6p<sup>56</sup>, all significant variant-gene cis eQTL pairs for whole blood, lung, and EBV-transformed lymphocytes were downloaded from <https://gtexportal.org>, and carried forward in analysis. From Westra et al.<sup>57</sup>, both cis and trans eQTLs in whole blood were downloaded, and variant-gene pairs with FDR < 0.1 were carried forward in analysis. From Fairfax et al.<sup>58</sup>, cis eQTLs from monocytes and B cells were downloaded, and variant-gene pairs with FDR < 0.1 were carried forward in analyses. From Bonder et al.<sup>58</sup>, meQTLs from whole blood were downloaded, and variant-probe pairs with FDR < 0.05 were carried forward in analyses. From Nicodemus-Johnson et al.<sup>59</sup>, cis eQTLs and meQTLs from lung were downloaded, and variant-gene pairs with FDR < 0.1 were carried forward in analyses. From Momozawa et al. [in press, personal correspondence], cis eQTLs from blood cell types CD14, CD15, CD19, CD4, and CD8 were downloaded, and variant-gene pairs with a weighted correlation of  $\geq 0.6$  were carried forward to analysis. For table 2 priority genes, protein coding information was downloaded from the UCSC Table Browser, using the “transcriptClass” field from the “wgEncodeGencodeAttrsV24lift37” table.

## Promoter Capture Hi-C Gene Prioritisation

To assess spatial promoter interactions in the discovery set, we performed a Capture Hi-C Gene Prioritisation (CHIGP) as described in Javierre et al.<sup>60</sup> and <https://github.com/ollyburren/CHIGP> using recommended settings and data sources: 0.1cM recombination blocks, 1KGP EUR reference population, coding markers from the GRCh37 Ensembl assembly and the CHICAGO-generated<sup>61</sup> Promoter Capture Hi-C peak matrix data from 17 human primary blood cell types supplied in the original paper. The resulting protein-coding prioritized genes (gene score > 0.5) were used in the downstream network analysis, from cell types "Fetal thymus", "Total CD4 T cells", "Activated total CD4 T cells", "Non-activated total CD4 T cells", "Naive CD4 T cells", "Total CD8 T cells", "Naive CD8 T cells", "Total B cells", "Naive B cells", "Endothelial precursors", "Macrophages M0", "Macrophages M1", "Macrophages M2", "Monocytes", and "Neutrophils".

## Gene set overrepresentation analysis of known and replicating novel loci

All high-confidence gene symbols from eQTL and meQTL sources, PCHiC, as well as genes (models extended 110kb upstream, and 40kb downstream) within each  $r^2$ -based loci definition from known and replicating novel loci were input into the pathway-based set over-representation analysis module of ConsensusPathDB (CPDB) database and tools<sup>62</sup> with 229 of 277 gene identifiers translated. In addition, these same symbols were used for Ingenuity pathway analysis (IPA; [www.ingenuity.com](http://www.ingenuity.com); a curated database of the relationships between genes obtained from published articles, and genetic and expression data repositories) to identify biological pathways common to genes. IPA determines whether the associated genes are significantly enriched in a

specific biological function or network by assessing direct interactions. We assigned significance if right-tailed Fisher's exact test p-value < 0.05. eQTL/meQTL, PCHiC and locus gene intersections were visualized using the UpSetR package<sup>63</sup>.

## Tissue overrepresentation

To assay the enrichment of variants associated with AR in tissue specific gene expression sets, we utilized the DEPICT enrichment method<sup>64</sup>, using a p-value threshold of 1e-5, and standard settings.

## Enrichment of regulatory regions

To assay the enrichment of variants associated with AR in regions of open chromatin and specific histone marks, we utilized the GWAS Analysis of Regulatory or Functional Information Enrichment with LD correction (GARFIELD) method<sup>65</sup>. In essence, GARFIELD performs greedy pruning of GWAS markers ( $LD\ r^2 > 0.1$ ) and then annotates them based on functional information overlap. Next, it quantifies Fold Enrichment (FE) at various GWAS significance cutoffs and assesses them by permutation testing, while adjusting for minor allele frequency, distance to nearest transcription start site and number of LD proxies ( $r^2 > 0.8$ ). GARFIELD was run with 10,000,000 permutations, and otherwise default settings.

## PARF

Population-attributable risk fractions (PARFs) were estimated from B58C, a general-population sample with participant ages 44-45 years also contributing to the discovery stage. The genetic risk score was calculated by applying the pooled per-allele coefficients ( $\ln(OR)$  values) from the AR discovery set to the number of higher-risk alleles of each of the 41 established (known genome-wide significant and novel replicated loci), one SNP per locus. Because there were no individuals observed with zero higher-risk alleles, the prevalence of sensitization for individuals in the lowest decile of the genetic risk score distribution was used to derive PARF estimates on the assumption that this 10% of the population was unexposed. This method has the advantage that it does not predict beyond the bounds of the data, but its results are conservative. The PARF was then derived (with 95% confidence interval) by expressing the difference between the observed prevalence and the predicted (unexposed) prevalence as a percentage of the observed prevalence. PARFs were estimated using the 41 AR loci in relation to AR, AS and NAR, respectively.

## Protein network and drug interactions

In order to analyse protein-protein-drug interaction networks, STRING (V10)<sup>66</sup> was used. Protein network data (9606.protein.links.v10.txt.gz) and protein alias data (9606.protein.alias.v10.txt) files were downloaded from the string db website [<http://string-db.org/>]. GWAS hits stratified on 'all', 'blood' and 'lung' were converted to Ensembl protein ids using the protein alias data. The interactors were subsequently identified using the link data at a 'high confidence cutoff of >0.7'

489 as described in the STRING FAQ. The interactor Ensembl protein ids were then converted to  
490 UniProt gene names and both hits and interactors were then analyzed for interactions with FDA  
491 approved drugs using the ChEMBL Database<sup>67</sup> API via Python (v2.7.12). Lastly, stratified  
492 networks consisting of GWAS hits connected to interactors and drugs connected to both GWAS  
493 hits and interactors were visualised using GGraph (v1.0.0), iGraph (v1.0.1), TidyVerse (v1.1.1)  
494 under R (v3.3.2).

## 495 Data availability

496 Genome-wide results are available on request through the corresponding author, on condition of  
497 signing any Data Transfer Agreements required according to the institutional review board  
498 (IRB)-approved protocols of contributing studies.  
499

## References

1. Greiner, A. N., Hellings, P. W., Rotiroti, G. & Scadding, G. K. Allergic rhinitis. *Lancet* **378**, 2112–2122 (2011).
2. Björkstén, B. *et al.* Worldwide time trends for symptoms of rhinitis and conjunctivitis: Phase III of the International Study of Asthma and Allergies in Childhood. *Pediatr. Allergy Immunol.* **19**, 110–124 (2008).
3. Willemsen, G., van Beijsterveldt, T. C. E. M., van Baal, C. G. C. M., Postma, D. & Boomsma, D. I. Heritability of self-reported asthma and allergy: a study in adult Dutch twins, siblings and parents. *Twin Res. Hum. Genet.* **11**, 132–142 (2008).
4. Fagnani, C. *et al.* Heritability and shared genetic effects of asthma and hay fever: an Italian study of young twins. *Twin Res. Hum. Genet.* **11**, 121–131 (2008).
5. Ramasamy, A. *et al.* A genome-wide meta-analysis of genetic variants associated with allergic rhinitis and grass sensitization and their interaction with birth order. *J. Allergy Clin. Immunol.* **128**, 996–1005 (2011).
6. Hinds, D. A. *et al.* A genome-wide association meta-analysis of self-reported allergy identifies shared and allergy-specific susceptibility loci. *Nat. Genet.* **45**, 907–911 (2013).
7. Bønnelykke, K. *et al.* Meta-analysis of genome-wide association studies identifies ten loci influencing allergic sensitization. *Nat. Genet.* **45**, 902–906 (2013).
8. Ferreira, M. A. R. *et al.* Genome-wide association analysis identifies 11 risk variants associated with the asthma with hay fever phenotype. *J. Allergy Clin. Immunol.* **133**, 1564–1571 (2014).
9. Bunyavanich, S. *et al.* Integrated genome-wide association, coexpression network, and expression single nucleotide polymorphism analysis identifies novel pathway in allergic rhinitis. *BMC Med. Genomics* **7**, 48 (2014).
10. Jahn-Schmid, B., Pickl, W. F. & Bohle, B. Interaction of Allergens, Major Histocompatibility



- 525       Complex Molecules, and T Cell Receptors: A ‘Ménage à Trois’ That Opens New Avenues  
526       for Therapeutic Intervention in Type I Allergy. *Int. Arch. Allergy Immunol.* **156**, 27–42  
527       (2011).
- 528   11. Cavalli, G. *et al.* MHC class II super-enhancer increases surface expression of HLA-DR  
529       and HLA-DQ and affects cytokine production in autoimmune vitiligo. *Proc. Natl. Acad. Sci.*  
530       *U. S. A.* **113**, 1363–1368 (2016).
- 531   12. Hayashi, M. *et al.* Autoimmune vitiligo is associated with gain-of-function by a  
532       transcriptional regulator that elevates expression of HLA-A\*02:01 in vivo. *Proc. Natl. Acad.*  
533       *Sci. U. S. A.* **113**, 1357–1362 (2016).
- 534   13. Puel, A., Ziegler, S. F., Buckley, R. H. & Leonard, W. J. Defective IL7R expression in T(-  
535       )B(+)NK(+) severe combined immunodeficiency. *Nat. Genet.* **20**, 394–397 (1998).
- 536   14. Lundmark, F. *et al.* Variation in interleukin 7 receptor alpha chain (IL7R) influences risk of  
537       multiple sclerosis. *Nat. Genet.* **39**, 1108–1113 (2007).
- 538   15. Mori, T. *et al.* Lnk/Sh2b3 controls the production and function of dendritic cells and  
539       regulates the induction of IFN- $\gamma$ -producing T cells. *J. Immunol.* **193**, 1728–1736 (2014).
- 540   16. Scott, L. M., Civin, C. I., Rorth, P. & Friedman, A. D. A novel temporal expression pattern of  
541       three C/EBP family members in differentiating myelomonocytic cells. *Blood* **80**, 1725–1735  
542       (1992).
- 543   17. Gao, H., Parkin, S., Johnson, P. F. & Schwartz, R. C. C/EBP gamma has a stimulatory role  
544       on the IL-6 and IL-8 promoters. *J. Biol. Chem.* **277**, 38827–38837 (2002).
- 545   18. León, B. *et al.* Regulation of T(H)2 development by CXCR5+ dendritic cells and  
546       lymphotoxin-expressing B cells. *Nat. Immunol.* **13**, 681–690 (2012).
- 547   19. Lawrence, T. The nuclear factor NF-kappaB pathway in inflammation. *Cold Spring Harb.*  
548       *Perspect. Biol.* **1**, a001651 (2009).
- 549   20. Shinnakasu, R. *et al.* Regulated selection of germinal-center cells into the memory B cell

- 550 compartment. *Nat. Immunol.* **17**, 861–869 (2016).
- 551 21. Roychoudhuri, R. *et al.* BACH2 regulates CD8(+) T cell differentiation by controlling access  
552 of AP-1 factors to enhancers. *Nat. Immunol.* **17**, 851–860 (2016).
- 553 22. Rothlin, C. V., Ghosh, S., Zuniga, E. I., Oldstone, M. B. A. & Lemke, G. TAM receptors are  
554 pleiotropic inhibitors of the innate immune response. *Cell* **131**, 1124–1136 (2007).
- 555 23. Chan, P. Y. *et al.* The TAM family receptor tyrosine kinase TYRO3 is a negative regulator  
556 of type 2 immunity. *Science* **352**, 99–103 (2016).
- 557 24. Kassmeier, M. D. *et al.* VprBP binds full-length RAG1 and is required for B-cell  
558 development and V(D)J recombination fidelity. *EMBO J.* **31**, 945–958 (2012).
- 559 25. Hamblet, C. E., Makowski, S. L., Tritapoe, J. M. & Pomerantz, J. L. NK Cell Maturation and  
560 Cytotoxicity Are Controlled by the Intramembrane Aspartyl Protease SPPL3. *J. Immunol.*  
561 **196**, 2614–2626 (2016).
- 562 26. Andersen, J. B., Strandbygård, D. J., Hartmann, R. & Justesen, J. Interaction between the  
563 2'-5' oligoadenylate synthetase-like protein p59 OASL and the transcriptional repressor  
564 methyl CpG-binding protein 1. *Eur. J. Biochem.* **271**, 628–636 (2004).
- 565 27. Halim, T. Y. F. *et al.* Retinoic-acid-receptor-related orphan nuclear receptor alpha is  
566 required for natural helper cell development and allergic inflammation. *Immunity* **37**, 463–  
567 474 (2012).
- 568 28. Anderson, D. M. *et al.* A homologue of the TNF receptor and its ligand enhance T-cell  
569 growth and dendritic-cell function. *Nature* **390**, 175–179 (1997).
- 570 29. Ferreira, M. A. *et al.* Shared genetic origin of asthma, hay fever and eczema elucidates  
571 allergic disease biology. *Nat. Genet.* **49**, 1752–1757 (2017).
- 572 30. Pearce, N., Pekkanen, J. & Beasley, R. How much asthma is really attributable to atopy?  
573 *Thorax* **54**, 268–272 (1999).
- 574 31. Bohme, M., Wickman, M., Lennart Nordvall, S., Svartengren, M. & Wahlgren, C. F. Family

575 history and risk of atopic dermatitis in children up to 4 years. *Clin. Exp. Allergy* **33**, 1226–  
576 1231 (2003).

577 32. Kreiner, E. *et al.* Shared genetic variants suggest common pathways in allergy and  
578 autoimmune diseases. *J. Allergy Clin. Immunol.* (2017). doi:10.1016/j.jaci.2016.10.055

579 33. Bousquet, J. *et al.* Important research questions in allergy and related diseases: nonallergic  
580 rhinitis: a GA2LEN paper. *Allergy* **63**, 842–853 (2008).

581 34. Moffatt, M. F. *et al.* Genetic variants regulating ORMDL3 expression contribute to the risk of  
582 childhood asthma. *Nature* **448**, 470–473 (2007).

583 35. Paternoster, L. *et al.* Multi-ancestry genome-wide association study of 21,000 cases and  
584 95,000 controls identifies new risk loci for atopic dermatitis. *Nat. Genet.* **47**, 1449–1456  
585 (2015).

586 36. Winkler, T. W. *et al.* Quality control and conduct of genome-wide association meta-  
587 analyses. *Nat. Protoc.* **9**, 1192–1212 (2014).

588 37. Mägi, R. & Morris, A. P. GWAMA: software for genome-wide association meta-analysis.  
589 *BMC Bioinformatics* **11**, 288 (2010).

590 38. Segrè, A. V. *et al.* Common inherited variation in mitochondrial genes is not enriched for  
591 associations with type 2 diabetes or related glycemic traits. *PLoS Genet.* **6**, (2010).

592 39. Karolchik, D. *et al.* The UCSC Table Browser data retrieval tool. *Nucleic Acids Res.* **32**,  
593 D493–6 (2004).

594 40. Subramanian, A. *et al.* Gene set enrichment analysis: a knowledge-based approach for  
595 interpreting genome-wide expression profiles. *Proc. Natl. Acad. Sci. U. S. A.* **102**, 15545–  
596 15550 (2005).

597 41. Yang, J., Lee, S. H., Goddard, M. E. & Visscher, P. M. GCTA: a tool for genome-wide  
598 complex trait analysis. *Am. J. Hum. Genet.* **88**, 76–82 (2011).

599 42. Chang, C. C. *et al.* Second-generation PLINK: rising to the challenge of larger and richer

600 datasets. *Gigascience* **4**, 7 (2015).

601 43. UK10K Consortium *et al.* The UK10K project identifies rare variants in health and disease.  
602 *Nature* **526**, 82–90 (2015).

603 44. Wellcome Trust Case Control Consortium *et al.* Bayesian refinement of association signals  
604 for 14 loci in 3 common diseases. *Nat. Genet.* **44**, 1294–1301 (2012).

605 45. McLaren, W. *et al.* The Ensembl Variant Effect Predictor. *Genome Biol.* **17**, 122 (2016).

606 46. Zheng, X. *et al.* HIBAG--HLA genotype imputation with attribute bagging.  
607 *Pharmacogenomics J.* **14**, 192–200 (2014).

608 47. Jia, X. *et al.* Imputing amino acid polymorphisms in human leukocyte antigens. *PLoS One*  
609 **8**, e64683 (2013).

610 48. Tian, C. *et al.* Genome-wide association and HLA region fine-mapping studies identify  
611 susceptibility loci for multiple common infections. *Nat. Commun.* **8**, (2017).

612 49. Berman, H. M. The Protein Data Bank. *Nucleic Acids Res.* **28**, 235–242 (2000).

613 50. Vita, R. *et al.* The immune epitope database (IEDB) 3.0. *Nucleic Acids Res.* **43**, D405–12  
614 (2015).

615 51. Sethi, D. K., Gordo, S., Schubert, D. A. & Wucherpfennig, K. W. Crossreactivity of a human  
616 autoimmune TCR is dominated by a single TCR loop. *Nat. Commun.* **4**, 2623 (2013).

617 52. Rückert, C. *et al.* Conformational dimorphism of self-peptides and molecular mimicry in a  
618 disease-associated HLA-B27 subtype. *J. Biol. Chem.* **281**, 2306–2316 (2006).

619 53. Bulik-Sullivan, B. *et al.* An atlas of genetic correlations across human diseases and traits.  
620 *Nat. Genet.* **47**, 1236–1241 (2015).

621 54. Zheng, J. *et al.* LD Hub: a centralized database and web interface to perform LD score  
622 regression that maximizes the potential of summary level GWAS data for SNP heritability  
623 and genetic correlation analysis. *Bioinformatics* **33**, 272–279 (2017).

624 55. Kettunen, J. *et al.* Genome-wide association study identifies multiple loci influencing human

625 serum metabolite levels. *Nat. Genet.* **44**, 269–276 (2012).

626 56. Lucas, A. O. Surveillance of communicable diseases in tropical Africa. *Int. J. Epidemiol.* **5**,  
627 39–43 (1976).

628 57. Westra, H.-J. *et al.* Systematic identification of trans eQTLs as putative drivers of known  
629 disease associations. *Nat. Genet.* **45**, 1238–1243 (2013).

630 58. Fairfax, B. P. *et al.* Genetics of gene expression in primary immune cells identifies cell type-  
631 specific master regulators and roles of HLA alleles. *Nat. Genet.* **44**, 502–510 (2012).

632 59. Nicodemus-Johnson, J. *et al.* DNA methylation in lung cells is associated with asthma  
633 endotypes and genetic risk. *JCI Insight* **1**, e90151 (2016).

634 60. Javierre, B. M. *et al.* Lineage-Specific Genome Architecture Links Enhancers and Non-  
635 coding Disease Variants to Target Gene Promoters. *Cell* **167**, 1369–1384.e19 (2016).

636 61. Cairns, J. *et al.* CHiCAGO: robust detection of DNA looping interactions in Capture Hi-C  
637 data. *Genome Biol.* **17**, 127 (2016).

638 62. Kamburov, A. *et al.* ConsensusPathDB: toward a more complete picture of cell biology.  
639 *Nucleic Acids Res.* **39**, D712–7 (2011).

640 63. Conway, J. R., Lex, A. & Gehlenborg, N. UpSetR: An R Package For The Visualization Of  
641 Intersecting Sets And Their Properties. (2017). doi:10.1101/120600

642 64. Pers, T. H. *et al.* Biological interpretation of genome-wide association studies using  
643 predicted gene functions. *Nat. Commun.* **6**, 5890 (2015).

644 65. Iotchkova, V. *et al.* GARFIELD - GWAS Analysis of Regulatory or Functional Information  
645 Enrichment with LD correction. *bioRxiv* 085738 (2016). doi:10.1101/085738

646 66. Szklarczyk, D. *et al.* STRING v10: protein-protein interaction networks, integrated over the  
647 tree of life. *Nucleic Acids Res.* **43**, D447–52 (2015).

648 67. Bento, A. P. *et al.* The ChEMBL bioactivity database: an update. *Nucleic Acids Res.* **42**,  
649 D1083–90 (2014).

# Table legends

## Table 1

Association results of index markers (variant with lowest p-value for each locus) from the discovery phase. Column “Nearest gene” denotes nearest up- and downstream gene (for intergenic variants with two genes listed), or surrounding gene (for intronic variants with one gene listed), with the exception of rs5743618, an exonic missense variant within *TLR1*; and rs1504215, an exonic synonymous variant within *BACH2*. Replication and combined p values are for a one-sided test.

## Table 2

Functional description of known and novel replicating loci. ‘Locus genes’ column denotes genes overlapping with R2-extended loci (See Methods). ‘Missense variant’ column denotes variants with a predicted missense coding consequences. ‘e/meQTL priority genes’ denotes genes prioritized from the combined e/meQTL analysis. ‘PCHiC priority genes’ denotes genes prioritized from the PCHiC chromatin capture analysis.  
a) Overlap for rs35350651 with group “other allergy” is “eosinophil count”, b) rs11671925 = eosinophilic esophagitis.

## Figure legends

### **Figure 1: Manhattan plot of the meta-GWAS discovery phase**

Circular plot of p-values of genetic marker association to allergic rhinitis from the discovery phase. Only markers with  $p < 1e-3$  are shown. Labels indicate nearest gene name for index marker in locus (marker with lowest p-value). Green labels indicate loci previously associated with allergy; blue labels indicate novel AR loci; grey labels indicate novel loci that were not carried forward to the replication phase. Green line indicates level of genome wide significance ( $p = 5e-8$ ).

### **Figure 2: Structural visualization of amino acid variants associated with allergic rhinitis**

The surface of the MHC molecules is shown in white, while the backbone of the bound peptides is shown in dark gray. The amino acid variant is highlighted in red and the peptide binding pockets of the MHC molecule is indicated with dashed circles. P1-P9 refers to positions in the peptides counting from the N-termini. (A) Localization of the strongest associated amino acid variant in HLA-DQB (MHC class II), HLA-DQB1 His30, located in the peptide binding pocket close to P6 of the peptide with a distance of 6Å (excluding peptide side chain). The protective amino acid variant at this location in relation to AR is His, whereas the risk variant is Ser. Histidine is positively charged and has a large aromatic ring, whereas Ser is not charged and not aromatic. Therefore, this mutation results in a significant change of the binding pocket environment. (B) Localization of the strongest associated amino acid variation in HLA-B (MHC class I), HLA-B AspHisLeu116, located close to P9 with a distance of 7Å (excluding peptide side chain). The close proximity to the bound peptide for both variants indicates that they are likely to affect the MHC-peptide interaction and thereby which peptides are presented.

### **Figure 3: Enrichment of allergic rhinitis-associated variants in tissue-specific open chromatin**

Enrichment of variants associated with allergic rhinitis (at  $p < 1e-08$  as threshold for marker association) in 189 cell types from ENCODE and Roadmap epigenomics data. Enrichment and p-value was calculated empirically against a permuted genomic background using the GARFIELD tool. Red labels indicate blood and blood-related cell-types, grey labels indicate other cell types. Due to number of permutations =  $1e7$ , empirical p-values reached a minimum ceiling of  $1/1e7$ . FDR threshold = 0.00026. For Epstein-Barr virus transformed B-lymphocyte cell types (cell type "GM\*\*\*\*"), only most enriched instance is shown ("B-Lymphocyte"). NHEK = normal human epidermal keratinocytes, HMEC/vHMEC = mammary epithelial cells, HCM = human cardiac myocytes, WI-38 = lung fibroblast-derived, HRGEC = human renal glomerular endothelial cell, HCFaa = Human Cardiac Fibroblasts-Adult Atrial cell, HMVEC-dBI-Neo = human microvascular endothelial cells, Th1 = T helper cell, type 1, Th2 = T helper cell, type 2.

### **Figure 4: Interaction network between drugs and proteins from genes associated with allergic rhinitis**

Grey nodes represent locus genes as well as genes prioritized from e/meQTL and PCHiC sources. Blue nodes represent drugs from the ChEMBL drug database. Edges represent very-



711 high confidence interactions from the STRING database (for locus-locus interactions) and drug  
712 target evidence (for drug-locus interactions). Red borders indicate genes with protein products  
713 that were significantly enriched in the “Th1 and Th2 Activation” pathway ( $-\log[p\text{-value}] > 19.1$ )  
714 from the IPA pathway analysis.

715

716

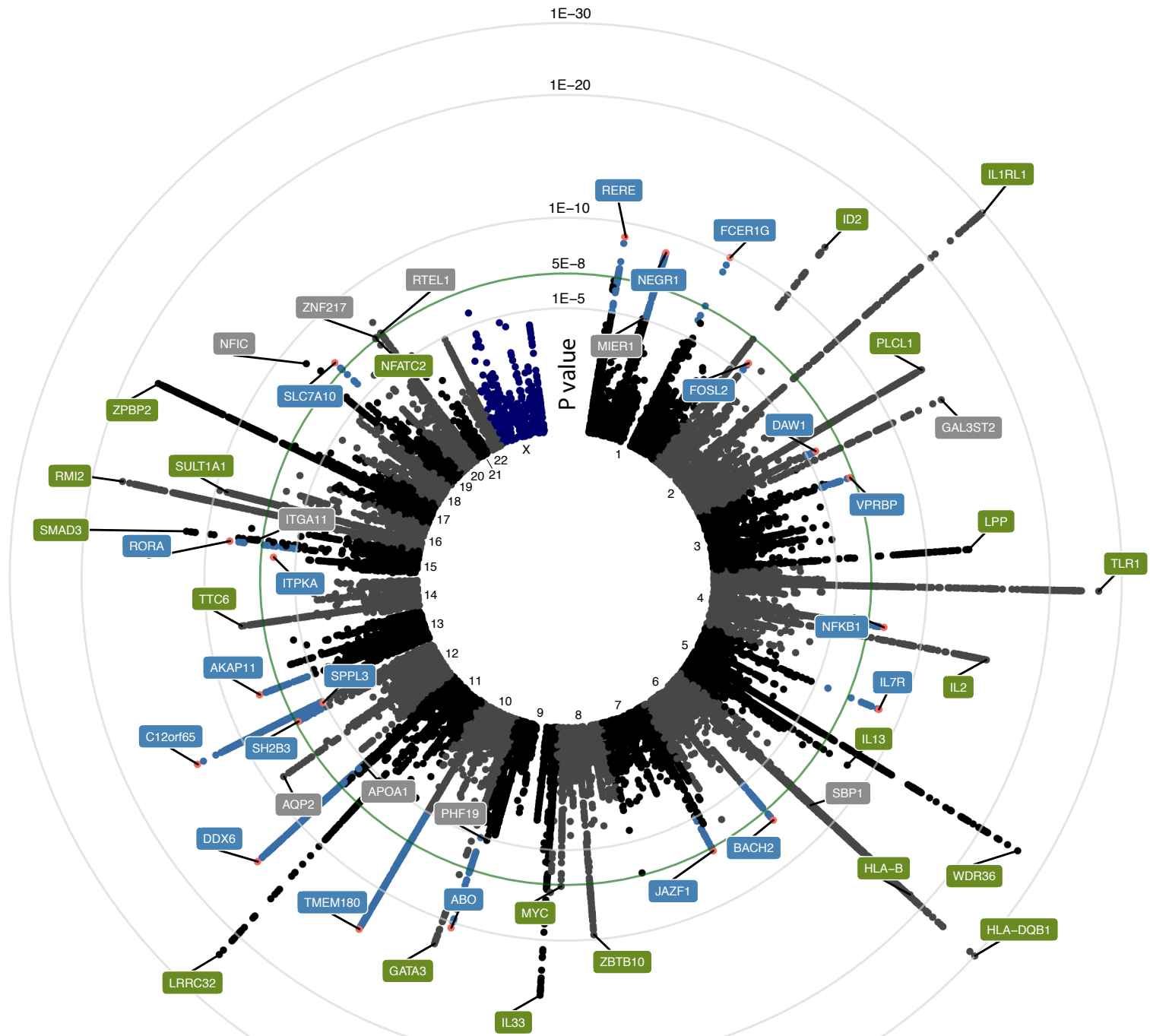
**Table 1.** Association results of index markers (variant with lowest p-value for each locus). Column “Nearest gene” denotes nearest up- and downstream gene (for intergenic variants with two genes listed), or surrounding gene (for intronic variants with one gene listed), with the exception of rs5743618, an exonic missense variant within *TLR1*; and rs1504215, an exonic synonymous variant within *BACH2*. Replication and combined p values are for a one-sided test. EA/OA=effect allele/other allele. P-value is calculated from the logistic regression model. Het.P=p-value for heterogeneity obtained from Cochrane’s Q test. \* Variants also reported associated with a combined asthma/eczema/hay fever phenotype by Ferreira et al.<sup>29</sup> (within +/- 1Mb).

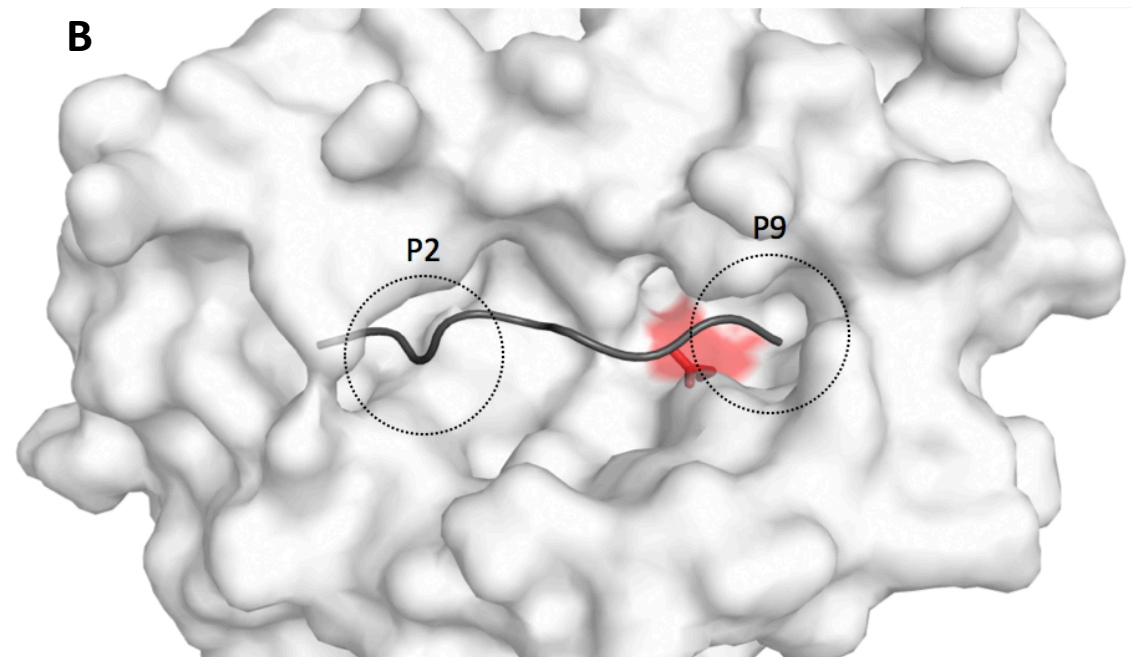
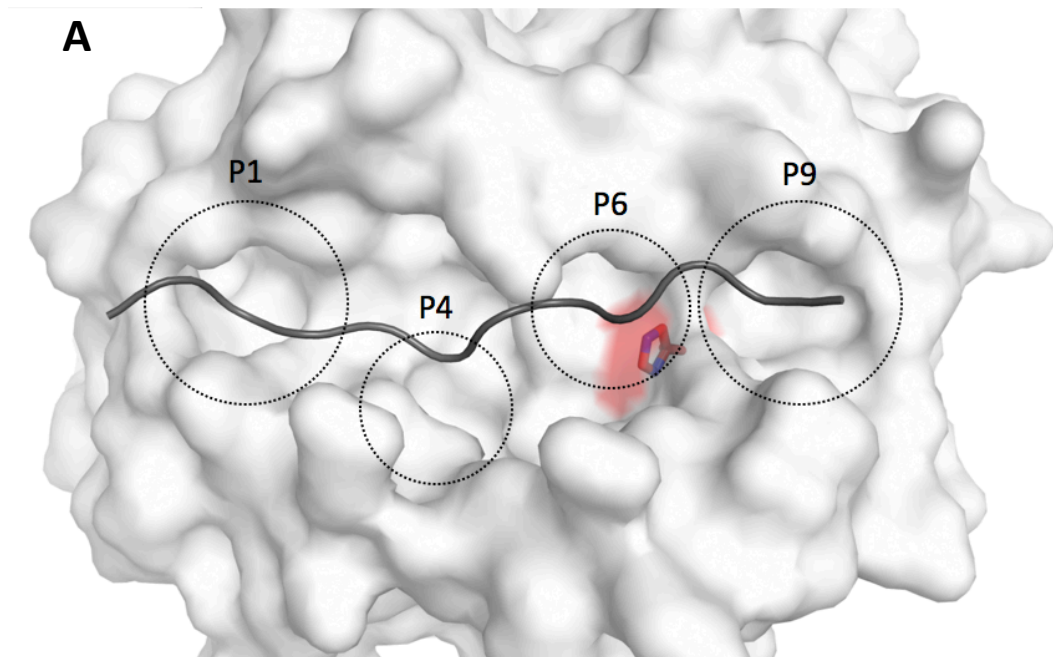
Variant	Locus	Nearest genes	EA/OA	Discovery					Het. P							
				EAF	n (studies)	OR [95% conf.int]	P									
Known																
rs34004019	6p21.32	HLA-DQB1;HLA-DQA1	G/A	0.27	196,951 (11)	0.89 [0.87-0.90]	1.00E-30	0.41								
rs950881	2q12.1	IL1RL1;IL1RL1	T/G	0.15	212,120 (18)	0.88 [0.87-0.90]	1.74E-30	0.91								
rs5743618	4p14	TLR1;TLR10	A/C	0.27	210,652 (17)	0.90 [0.89-0.92]	4.38E-27	0.70								
rs1438673	5q22.1	CAMK4;WDR36	C/T	0.50	212,120 (18)	1.08 [1.07-1.10]	3.15E-26	0.26								
rs7936323	11q13.5	LRRC32;C11orf30	A/G	0.48	212,120 (18)	1.08 [1.06-1.09]	6.53E-24	0.0001								
rs2428494	6p21.33	HLA-B;HLA-C	A/T	0.42	195,753 (12)	1.08 [1.06-1.09]	7.01E-19	0.25								
rs11644510	16p13.13	RMI2;CLEC16A	T/C	0.37	212,120 (18)	0.93 [0.92-0.95]	1.58E-17	0.65								
rs12939457	17q12	GSDMB;ZPBP2	C/T	0.44	212,120 (18)	0.94 [0.92-0.95]	2.35E-17	0.02								
rs148505069	4q27	IL21;IL2	G/A	0.33	212,120 (18)	1.07 [1.05-1.08]	2.54E-15	0.02								
rs13395467	2p25.1	ID2;RNF144A	G/A	0.28	212,120 (18)	0.94 [0.92-0.95]	9.93E-15	0.61								
rs9775039	9p24.1	IL33;RANBP6	A/G	0.16	212,120 (18)	1.08 [1.06-1.10]	2.22E-14	0.40								
rs2164068	2q33.1	PLCL1	A/T	0.49	212,120 (18)	0.94 [0.93-0.96]	4.21E-14	0.82								
rs2030519	3q28	TPRG1;LPP	G/A	0.49	212,120 (18)	1.06 [1.04-1.07]	1.83E-13	0.12								
rs11256017	10p14	CELF2;GATA3	T/C	0.18	212,120 (18)	1.07 [1.05-1.09]	2.72E-12	0.60								
rs17294280	15q22.33	AAGAB;SMAD3	G/A	0.25	212,120 (18)	1.07 [1.05-1.09]	5.97E-12	0.07								
rs7824993	8q21.13	ZBTB10;TPD52	A/G	0.37	212,120 (18)	1.05 [1.04-1.07]	1.86E-10	0.56								
rs9282864	16p11.2	SULT1A1;SULT1A2	C/A	0.33	208,761 (16)	0.94 [0.93-0.96]	4.69E-10	0.03								
rs9687749	5q31.1	IL13;RAD50	T/G	0.44	207,604 (16)	1.06 [1.04-1.09]	1.84E-09	0.19								
rs61977073	14q21.1	TTC6	G/A	0.22	212,120 (18)	1.06 [1.04-1.08]	5.78E-09	0.05								
rs6470578	8q24.21	TMEM75;MYC	T/A	0.28	212,120 (18)	1.05 [1.03-1.07]	4.36E-08	0.02								
rs3787184	20q13.2	NFATC2;KCNG1	G/A	0.19	207,604 (16)	0.94 [0.93-0.96]	4.76E-08	0.69								
Novel						Replication				Combined						
						n (studies)	OR [95% conf.int]	P	FWER	n (studies)	OR [95% conf.int]	P	Het. P			
rs7717955*	5p13.2	CAPSL;IL7R	T/C	0.27	212,120 (18)	0.95 [0.93-0.96]	1.50E-09	0.24	679,247 (10)	0.93 [0.91-0.94]	4.09E-25	1.06E-23	891,367 (28)	0.94 [0.93-0.95]	3.78E-32	0.09
rs63406760*	12q24.31	CDK2AP1;C12orf65	G/-	0.26	210,652 (17)	0.93 [0.91-0.95]	5.12E-14	0.91	675,338 (7)	0.95 [0.93-0.96]	3.27E-12	8.51E-11	885,990 (24)	0.94 [0.93-0.95]	2.54E-24	0.89
rs1504215*	6q15	BACH2;GJA10	A/G	0.34	207,604 (16)	0.95 [0.94-0.97]	1.49E-08	0.02	679,247 (10)	0.95 [0.94-0.97]	1.99E-11	5.17E-10	886,851 (26)	0.95 [0.94-0.96]	1.54E-18	0.05
rs28361986*	11q23.3	CXCR5;DDX6	A/T	0.20	212,120 (18)	0.93 [0.91-0.95]	1.81E-14	0.87	675,919 (8)	0.94 [0.93-0.96]	7.92E-11	2.06E-09	888,039 (26)	0.94 [0.92-0.95]	2.32E-23	0.91
rs2070902*	1q23.3	AL590714.1;FCER1G	T/C	0.25	212,120 (18)	1.06 [1.04-1.08]	1.03E-10	0.18	679,247 (10)	1.05 [1.03-1.06]	7.27E-10	1.89E-08	891,367 (28)	1.05 [1.04-1.06]	6.19E-19	0.23
rs111371454*	15q15.1	ITPKA;RTF1	G/A	0.21	212,120 (18)	1.06 [1.03-1.08]	1.65E-07	0.17	675,338 (7)	1.04 [1.03-1.06]	8.47E-09	2.20E-07	887,458 (25)	1.05 [1.03-1.06]	1.28E-14	0.22
rs12509403*	4q24	MANBA;NFKB1	T/C	0.32	212,120 (18)	0.95 [0.94-0.97]	9.97E-09	0.27	679,247 (10)	0.96 [0.95-0.97]	1.86E-08	4.84E-07	891,367 (28)	0.96 [0.95-0.97]	1.17E-15	0.39
rs9648346*	7p15.1	JAZF1;TAX1BP1	G/C	0.22	207,604 (16)	1.05 [1.03-1.07]	3.62E-08	0.74	679,247 (10)	1.04 [1.03-1.06]	1.39E-07	3.63E-06	886,851 (26)	1.05 [1.03-1.06]	3.30E-14	0.48
rs35350651*	12q24.12	ATXN2;SH2B3	C/-	0.49	206,136 (15)	1.04 [1.03-1.06]	6.63E-08	0.60	672,701 (6)	1.04 [1.02-1.05]	1.41E-07	3.66E-06	878,837 (21)	1.04 [1.03-1.05]	5.82E-14	0.43
rs2519093*	9q34.2	ABO;OBP2B	T/C	0.20	212,120 (18)	1.06 [1.04-1.09]	4.96E-11	0.38	675,919 (8)	1.04 [1.03-1.06]	2.96E-07	7.68E-06	888,039 (26)	1.05 [1.04-1.07]	2.79E-16	0.61
rs62257549	3p21.2	VPRBP	A/G	0.20	212,120 (18)	0.95 [0.93-0.97]	7.13E-08	0.45	677,615 (9)	0.96 [0.94-0.97]	3.37E-07	8.76E-06	889,735 (27)	0.95 [0.94-0.97]	1.84E-13	0.53
rs11677002	2p23.2	FOSL2;RBKS	C/T	0.45	212,120 (18)	0.96 [0.95-0.98]	3.80E-07	0.21	679,247 (10)	0.97 [0.96-0.98]	3.54E-07	9.20E-06	891,367 (28)	0.97 [0.96-0.97]	7.08E-13	0.36
rs35597970*	10q24.32	ACTR1A;TMEM180	-/A	0.45	210,652 (17)	1.06 [1.04-1.07]	1.34E-13	0.96	676,970 (8)	1.03 [1.02-1.05]	4.37E-07	1.14E-05	887,622 (25)	1.04 [1.03-1.05]	5.42E-18	0.53
rs2815765	1p31.1	LRRIQ3;NEGR1	T/C	0.37	212,120 (18)	0.95 [0.94-0.97]	1.18E-09	0.59	679,247 (10)	0.97 [0.95-0.98]	6.16E-07	1.60E-05	891,367 (28)	0.96 [0.95-0.97]	9.45E-15	0.52
rs11671925*	19q13.11	CEBPA;SLC7A10	A/G	0.17	206,136 (15)	0.94 [0.92-0.96]	1.80E-08	0.97	677,551 (9)	0.96 [0.94-0.98]	2.80E-06	7.29E-05	883,687 (24)	0.95 [0.94-0.96]	5.91E-13	0.60
rs2461475*	12q24.31	SPPL3;ACADS	C/T	0.47	212,120 (18)	1.04 [1.02-1.05]	9.19E-07	0.97	677,551 (9)	1.03 [1.02-1.04]	6.52E-06	0.0002	889,671 (27)	1.03 [1.02-1.04]	3.81E-11	0.83
rs6738964*	2q36.3	SPHKAP;DAW1	G/T	0.24	212,120 (18)	0.96 [0.94-0.97]	4.51E-07	0.72	679,247 (10)	0.97 [0.96-0.98]	4.96E-05	0.0013	891,367 (28)	0.96 [0.95-0.97]	1.86E-10	0.87
rs10519067*	15q22.2	RORA	A/-	0.13	212,120 (18)	0.93 [0.91-0.96]	1.78E-09	0.37	442,354 (7)	0.93 [0.90-0.96]	7.53E-05	0.0020	654,474 (25)	0.93 [0.92-0.95]	5.53E-13	0.36
rs138050288*	1p36.23	RERE;SLC45A1	-/CA	0.29	210,652 (17)	1.05 [1.04-1.07]	5.96E-10	0.71	675,338 (7)	1.03 [1.01-1.04]	0.0002	0.0046	885,990 (24)	1.04 [1.03-1.05]	6.62E-12	0.63
rs7328203	13q14.11	TNFSF11;AKAP11	G/T	0.46	212,120 (18)	1.05 [1.03-1.06]	5.94E-09	0.90	677,551 (9)	1.02 [1.01-1.04]	0.0005	0.0134	889,671 (27)	1.03 [1.02-1.04]	1.28E-10	0.78

**Table 2.** Functional description of known and novel replicating loci. ‘Locus genes’ column denotes genes overlapping with R2-extended loci (See Methods). ‘Missense variant’ column denotes variants with a predicted missense coding consequences. ‘e/meQTL priority genes’ denotes genes prioritized from the combined e/meQTL analysis. ‘PCHiC priority genes’ denotes genes prioritized from the PCHiC chromatin capture analysis. \* Variants also reported associated with a combined asthma/eczema/hay fever phenotype by Ferreira et al.<sup>29</sup> (within +/- 1Mb).

Variant	Locus	Locus genes	Missense variant	e/meQTL priority genes	PCHiC priority genes	Possible function
<b>Known</b>						
rs13395467	2p25.1				<b>ID2</b>	Transcription factor required for specific innate cell, T cell and B cell subsets
rs950881	2q12.1	<b>IL1RL1</b> , IL18R1, IL18RAP		IL18R1, IL18RAP, <b>IL1RL1</b> , MFSD9	<b>IL1RL1</b>	Interleukin receptor, IL33-signalling, Th2-response
rs2164068	2q33.1	<b>PLCL1</b>	PLCL1	COQ10B, MARS2, <b>PLCL1</b> , RFTN2, SF3B1	<b>PLCL1</b>	Phospholipase, intracellular signalling
rs2030519	3q28	<b>LPP</b>				Transcription factor, Th2-differentiation
rs5743618	4p14	<b>TLR10</b> , <b>TLR1</b> , <b>TLR6</b> , FAM114A1	TLR1	FAM114A1, <b>TLR1</b> , <b>TLR10</b> , <b>TLR6</b>		Pattern recognition receptors, innate immunity
rs148505069	4q27	IL2		<b>IL21</b>		Interleukin, immune regulatory effects
rs1438673	5q22.1	WDR36, CAMK4		<b>TSLP</b>		Th2 immune responses
rs9687749	5q31.1	<b>IL13</b> , IL4, IL5, RAD50	<b>IL13</b>			Interleukin, IgE secretion, allergic inflammation
rs34004019	6p21.32	HLA-DRB1, HLA-DQB1, HLA-DQA2, HLA-DQA1		C4A, CYP21A2, <b>HLA-DOB</b> , HLA-DQA1, HLA-DQA2, HLA-DQB1, HLA-DQB2, HLA-DRA, HLA-DRB1, HLA-DRB5, LY6G5B, TAP2		Antigen presentation, self tolerance
rs2428494	6p21.33	<b>MICA</b> , HLA-B, HLA-C		C4A, HCG27, <b>MICA</b>		Stress induced ligand recognized by NK and T cells
rs7824993	8q21.13				MRPS28	Unknown
rs6470578	8q24.21			<b>MYC</b>		Transcription factor, B-cell proliferation and differentiation
rs9775039	9p24.1	<b>IL33</b>		<b>CD274</b>		IL33: Interleukin, Th2-signalling. CD274: Immune regulation
rs11256017	10p14					
rs7936323	11q13.5	C11orf30, <b>LRRC32</b>				Treg expressed, TGF-beta signalling
rs61977073	14q21.1	TTC6, <b>FOXA1</b>	<b>FOXA1</b>			Transcription factor, Treg differentiation
rs17294280	15q22.33	<b>SMAD3</b> , IQCH, AAGAB		<b>SMAD3</b>	<b>SMAD3</b>	Transcriptional factor, TGF-beta signalling
rs9282864	16p11.2	EIF3C, <b>IL27</b> , NPIP8, NUPR1, SGF29, SULT1A1, SULT1A2		APOBR, ATXN2L, CLN3, EIF3C, EIF3CL, <b>IL27</b> , NPIP8, NPIP7, SBK1, SH2B1, SPNS1, SULT1A1, SULT1A2, TUFM		Induces naïve T cell proliferation and Th1 differentiation while suppressing Th17, Th2 and Treg responses. Induces isotype swithcing of B cells and has additional effects on innate immune cells.
rs11644510	16p13.13	RMI2, CLEC16A		<b>DEXI</b>	C16orf72, CLEC16A, <b>DEXI</b> , GSPT1, LITAF, NUBP1, PRM2, PRM3, RMI2, RSL1D1, SNN, SOCS1, TNP2, TXNDC11, ZC3H7A	Unknown function. Highly expressed in lung, B- and T-cells
rs12939457	17q12	GSDMA, GSDMB, IKZF3, LRRC3C, PSMD3, ZPBP2	GSDMB, ZPBP2	GSDMA, GSDMB, IKZF3, MED24, ORMDL3, PGAP3, ZPBP2	GSDMB, <b>ORMDL3</b>	Regulator of sphingolipid synthesis. Endoplasmic reticulum-mediated Ca(+2) signaling
rs3787184	20q13.2	<b>NFATC2</b>				Transcription factor, activated T-cell gene transcription

Variant	Locus	Locus genes	Missense variant	e/meQTL priority genes	PCHiC priority genes	Possible function
<b>Novel, replicating</b>						
rs2815765	1p31.1	<b>NEGR1</b>		<b>NEGR1</b>		Cell adhesion.
rs138050288*	1p36.23	<b>RERE</b>		<b>RERE</b>		Transcription factor associated with apoptosis.
rs2070902*	1q23.3	ADAMTS4, AL590714.1, APOA2, B4GALT3, DEDD, <b>FCER1G</b> , NDUFS2, NR1I3, PCP4L1, PFDN2, SDHC, TOMM40L		<b>FCER1G</b> , TOMM40L, USF1		Codes for the high affinity IgE receptor involved in allergic responses. Present on many cell types, including immune cells and epithelial cells.
rs11677002	2p23.2	<b>FOSL2</b> , PLB1		<b>FOSL2</b>		Cell cycle and proliferation.
rs6738964*	2q36.3	<b>DAW1</b>				Dynein assembly factor.
rs62257549	3p21.2	<b>VPRBP</b> , RAD54L2		HYAL3, MAPKAPK3, NAT6, RBM15B		Required for optimal T cell proliferation after antigen encounter and involved in V(D)J recombination during B cell development.
rs12509403*	4q24	<b>NFKB1</b> , MANBA		BDH2, MANBA, <b>NFKB1</b>		NFKB1: Activation of multiple inflammatory pathways, mediating signals from toll-like receptors and cytokines.
rs7717955*	5p13.2	<b>IL7R</b>	<b>IL7R</b>	<b>IL7R</b> , LMBRD2, SPEF2, UGT3A2		Necessary for V(D)J recombination of T and B cell receptors. T cell sub-populations have different levels of IL-7R on the cell surface.
rs1504215*	6q15	<b>BACH2</b>		<b>BACH2</b>	<b>BACH2</b>	Role in several immune cells, including antigen-induced formation of memory B cells and memory T cells.
rs9648346*	7p15.1	<b>JAZF1</b>		CREB5, <b>JAZF1</b>		Transcriptional repressor, associated with systemic sclerosis, type 2 diabetes and endometrial stromal tumors.
rs2519093*	9q34.2	ABO, GBGT1, OBP2B, RPL7A, STKLD1, SURF2		<b>ABO</b> , GBGT1, MED22, SURF1, SURF4, SURF6		Allelic variants of ABO determine blood group type.
rs35597970*	10q24.32	CUEDC2, PSD, TMEM180, ACTR1A, SUFU		ACTR1A, ARL3, AS3MT, SUFU, TMEM180, TRIM8	<b>NFKB2</b>	Subunit of NFKB complex which is expressed in many cell types and involved in regulating immune responses, including TLR-4 and cytokine signaling.
rs28361986*	11q23.3	DDX6, <b>CXCR5</b>		<b>CXCR5</b> , TRAPPC4	<b>CXCR5</b> , DDX6	Chemokine receptor present on B cells and involved in B cell migration to the B cell follicular zone in lymph nodes and spleen; CXCR5 is also expressed on a subset of follicular T cells.
rs35350651*	12q24.12	<b>SH2B3</b> , FAM109A, ATXN2	<b>SH2B3</b> SBNO1	ALDH2, <b>SH2B3</b> , TMEM116		Involved in hematopoiesis as well as downstream of T cell receptor activation.
rs63406760*	12q24.31	C12orf65, CDK2AP1, MPHOSPH9, SBNO1		ABCB9, ARL6IP4, C12orf65, CDK2AP1, MPHOSPH9, OGFOD2, PITPNM2, RILPL2, SBNO1, SETD8, SNRNP35 C12orf43, <b>OASL</b> , RNF10, <b>SPPL3</b>	<b>DDX55</b>	DDX55: Involved in multiple nuclear processes.
rs2461475*	12q24.31	<b>SPPL3</b>				SPPL3: Deletion results in decreased numbers of NK cells. OASL: Involved in IFN-gamma signaling.
rs7328203	13q14.11	<b>TNFSF11</b> , AKAP11		AKAP11		Enhances T cell activation by dendritic cells.
rs111371454*	15q15.1	ITPKA, NDUFAF1, RTF1, <b>TYRO3</b> , <b>LTK</b>	NDUFAF1, NUSAP1	ITPKA, <b>LTK</b> , NDUFAF1, OIP5, RPAP1		TYRO3: Inhibits TLR-mediated immune signaling and activates SOCS1 (identified as potential gene in previous screen). LTK: Leukocyte tyrosine kinase that is involved in downstream T cell receptor signalling.
rs10519067*	15q22.2	<b>RORA</b>			<b>CEBPA</b> , <b>CEBPG</b>	Involved natural helper cell development and allergic disease.
rs11671925	19q13.11	SLC7A10, LRP3				CEBPA: Important for lung development. Associated with inflammatory bowel disease. CEBPG: Transcriptional enhancers for the immunoglobulin heavy chain.





$-\log_{10}[\text{Empirical p-value}]$

